Formation and shape control of InAsSb/InP (001) nanostructures

W. Lei, H. H. Tan, and C. Jagadish

Citation: Appl. Phys. Lett. **95**, 013108 (2009); doi: 10.1063/1.3160738
View online: http://dx.doi.org/10.1063/1.3160738
View Table of Contents: http://apl.aip.org/resource/1/APPLAB/v95/i1
Published by the American Institute of Physics.

Formation and shape control of InAsSb/InP (001) nanostructures

W. Lei,[a] H. H. Tan, and C. Jagadish
Department of Electronic Materials Engineering, Research School of Physics and Engineering, The Australian National University, Canberra, Australian Capital Territory 0200, Australia

(Received 30 April 2009; accepted 9 June 2009; published online 7 July 2009)

This paper presents a study on the formation and shape control of InAsSb/InP nanostructures on InP (001) substrates. For the formation of InAsSb nanostructures, incorporation of Sb atoms into InAs islands results in significant morphology change in the islands due to the surfactant effect of Sb atoms and the large strain in the system. And, shape control of InAsSb/InP nanostructures is achieved by optimizing their growth parameters. Low growth temperature and high growth rate will induce the formation of InAsSb elongated quantum dots, while high growth temperature and low growth rate will promote the formation of InAsSb quantum wires or dashes. © *2009 American Institute of Physics*. [DOI: 10.1063/1.3160738]

Semiconductor nanostructures, such as quantum dots (QDs), quantum dashes (QDashes), and quantum wires (QWRs), have attracted wide attention due to their applications in devices.[1,2] Most of the work on QDs and QWRs are focused on GaAs- and InP-based In(Ga)As nanostructures with the target at 1.3 and 1.55 μm emission wavelength.[3,4] Recently, much attention has been devoted to extending the emission wavelength of InP-based InAs nanostructures into 1.8–3 μm region due to their use in military, telecommunications, molecular spectroscopy, biomedical surgery, environmental protection, and manufacturing industry applications. However, it is very hard to extend the emission wavelength of InP-based In(Ga)As nanostructures above 2 μm due to the limitation of InAs/InP material system.

Incorporating some antimony (Sb) into InAs nanostructures to form InAsSb nanostructures provides a very promising way to achieve the 2–3 μm emission wavelength. Theoretical calculations showed that the emission wavelength of InP-based InAsSb QDs can be extended into the 2–3 μm range, even reaching 5 μm.[5] However, because of the difficulty in growing antimony compounds, limited experimental work has been done on the growth of InAsSb QDs on InP substrates.[6–10] In this paper, we investigate the growth and shape control of InAsSb/InP nanostructures on InP (001) substrates. The growth parameters of InAsSb nanostructures such as growth temperature and growth rate are demonstrated to be important factors to achieve the controlled growth of InAsSb/InP nanostructures.

InAs(Sb)/InP nanostructures were grown on semi-insulating InP (001) substrates using a horizontal flow metal-organic chemical-vapor deposition reactor (AIX200/4) at a pressure of 180 mbar. Trimethylindium, trimethylgallium, trimethylantimony (TMSb), PH_3, and AsH_3 were used as precursors, and ultrahigh purity H_2 as the carrier gas. For reference, an InAs/InP QD sample was grown. The InAs/InP QD sample was grown using the following layer sequence: first, a 200 nm InP buffer was deposited at 650 °C, then a 0.6 nm GaAs interlayer was grown at 650 °C to suppress the As–P exchange, then the growth temperature (T_g) was reduced to 520 °C to grow 4 ML InAs QD layer at a growth rate (R_g) of 0.5 ML/s and a V/III ratio of 15,[11] then the InAs QDs were capped immediately without any growth interruption with a 100 nm InP cap layer while the growth temperature is ramped up to 650 °C. The same steps were followed to grow a top layer of InAs QDs for atomic force microscopy (AFM) measurements. The InAsSb/InP nanostructure samples had the same growth sequence as the InAs/InP QD samples. During the growth of InAsSb nanostructures, the valve of TMSb source had the same on and off sequence as that of AsH_3 source, which allowed both As and Sb atoms to bond with In atom terminated surface simultaneously, and form an InAsSb layer (different from the "Sb-protected annealing" growth method in Refs. 7 and 8, where the morphology of InAsSb islands is mainly influenced by that of InAs islands formed). The InAsSb nanostructures had a nominal composition of $InAs_{0.5}Sb_{0.5}$. A typical V/III ratio of 1.5 was applied for the growth of InAsSb nanostructures.[12] To study the effect of T_g and R_g on the morphology of InAsSb nanostructures, T_g of InAsSb layers was varied from 500 to 540 °C, and R_g of InAsSb layers varied from 0.33 to 1.17 ML/s. The morphology of top InAs(Sb) nanostructures was characterized by using AFM in tapping mode. The photoluminescence (PL) spectra of the samples were measured at 77 K under excitation by a 635 nm laser line. The luminescence signal was collected by a liquid nitrogen cooled extended InGaAs photodetector.

Figures 1(a) and 1(b) show the typical AFM images of the InAs/InP and InAsSb/InP nanostructures grown at a R_g of 0.5 ML/s at 520 °C. It is observed that elongated QDs are formed in the InAs/InP sample. The InAs QDs are, on average, 8 nm in height, 30 nm in width, and 55 nm in length. The areal density of InAs QDs is around 1.34×10^{10} cm^{-2}. In contrast, flat QDashes with higher density are formed in the InAsSb/InP sample. The InAsSb QDashes are elongated along the $[1\bar{1}0]$ direction with a mean height of 1.7 nm, width (along the [110] direction) of 25 nm, and length (along the $[1\bar{1}0]$ direction) of 105 nm, respectively. This morphology change after incorporating Sb atoms into InAs QDs has also been noted in previous works.[9,10] The formation of flat InAsSb QDashes can be mainly attributed to the surfactant effect of Sb atoms in the structures.[9,10,13–15] According to previous reports,[9,10] some Sb atoms in InAsSb structures deposited will segregate to the surface, and the resultant Sb-stabilized surface prefers to lower its surface energy by

[a]Electronic mail: wen.lei@anu.edu.au.

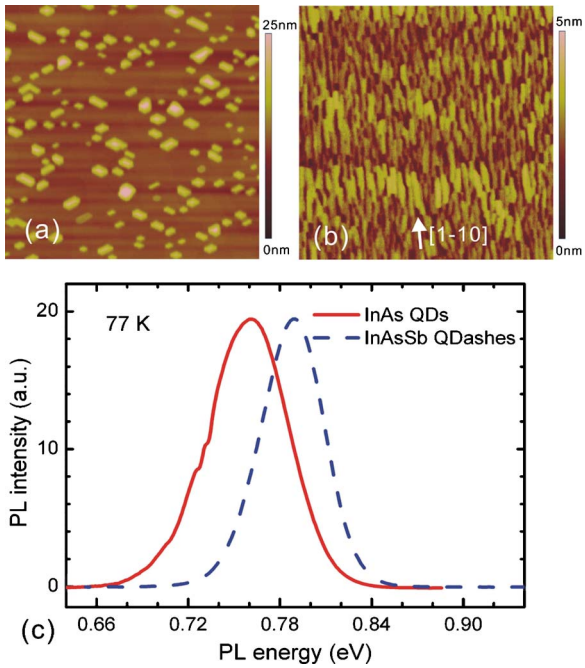

FIG. 1. (Color online) Typical AFM images of (a) InAs/InP QDs and (b) InAsSb/InP QDashes, and (c) 77 K PL spectra of the InAs/InP QDs and InAsSb/InP QDashes. AFM scan size is 1 μm^2.

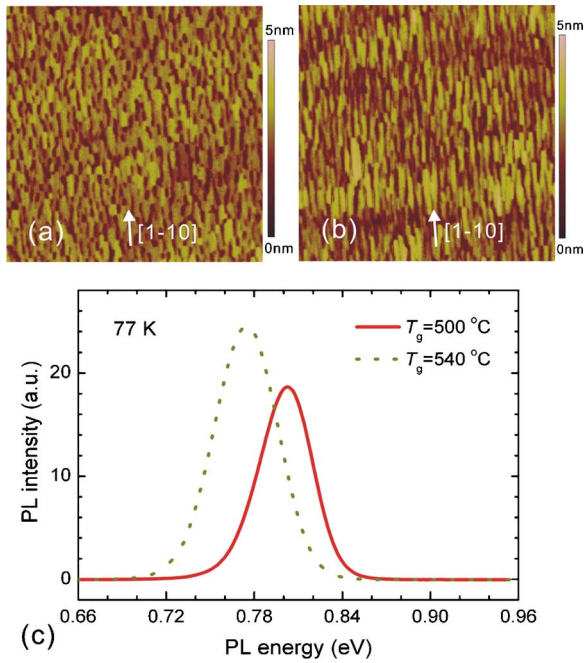

FIG. 2. (Color online) Typical AFM images of InAsSb/InP nanostructures grown under (a) 500 and (b) 540 °C, and (c) 77 K PL spectra of the InAsSb/InP nanostructures grown under 500 and 540 °C. AFM scan size is 1 μm^2.

forming flat islands with large areas.[13,14] Theoretically, to reach minimum energy in the system, an anisotropic shape (wire or dash) is more stable for quantum structures with large areas when the InAsSb island size exceeds its equilibrium size α_0. Also, the most stable anisotropic shape requires that the lateral size of the islands equals to the equilibrium size α_0.[15] This leads to the formation of dash or wire structures for InAsSb/InP system. The alignment of InAsSb QDashes along the $[1\bar{1}0]$ direction can be ascribed to the large migration length of In adatoms along the $[1\bar{1}0]$ direction induced by surface anisotropy. The decreased width in InAsSb QDashes can be mainly attributed to the increased strain in InAsSb/InP system compared with InAs/InP system. In addition, the reduced migration length of In adatoms induced by Sb atoms in wetting layer also contributes to the decreased width in InAsSb QDashes. The 77 PL spectra of the two samples are shown in Fig. 1(c). The PL peak of InAs QDs and InAsSb QDashes are centered at 0.762 and 0.793 eV, respectively. Obviously, the introduction of Sb atoms into InAs QDs induces a 31 meV blueshift for the PL peak, which can be attributed to the small height of InAsSb QDashes.

To achieve InAsSb QDs, some approaches should be taken to reduce the migration length of In adatoms along the $[1\bar{1}0]$ direction, which could be achieved by optimizing the T_g and R_g of InAsSb layers.[16–18] Figures 2(a) and 2(b) show the typical AFM images of InAsSb nanostructures grown at a R_g of 0.5 ML/s under 500 and 540 °C. Combined with Fig. 1(b), it is observed that the aspect ratio (length/width) of InAsSb islands changes significantly with increasing T_g, while their heights only vary a little. The InAsSb islands show a mean height of 1.3 and 2 nm for the samples grown at 500 and 540 °C, respectively. However, when the T_g of InAsSb layers increases from 500 to 540 °C, the average length of InAsSb islands increases significantly from 70 to 130 nm, while the average widths of InAsSb islands are all around 25 nm. The reason for the almost identical average width of InAsSb islands with increasing T_g is not well understood. The evolution of InAsSb island length with increasing T_g can be explained by the kinetic characteristics of the Stranski–Krastanov (SK) growth.[16,17] In SK growth, In adatoms deposited after island formation will prefer to be incorporated into existing islands rather than form new islands, as they are energetically favorable. Meanwhile, the T_g change has a significant influence on the migration length of In adatoms. At high T_g such as 540 °C, the In adatoms have relatively larger migration length, and thus easily reach the existing small islands and get absorbed, leading to the formation of long QDash structures with relatively large size, large size fluctuation, and low density. Instead, at low T_g such as 500 °C, the In adatoms will have relatively small migration length, and thus have more chance to form new islands, resulting in the formation of elongated QDs or short QDashes with relatively small size, small size fluctuation, and high density. This morphology evolution of InAsSb nanostructures with increasing T_g is further confirmed by the PL measurements. Figure 2(c) shows the 77 PL spectra of the two samples grown under 500 and 540 °C. Combined with Fig. 1(c), it is observed that the PL peaks are centered at 0.803, 0.793, and 0.775 eV with a full width at half maximum (FWHM) of 42, 48, and 52 meV for InAsSb nanostructures obtained at 500, 520, and 540 °C, respectively. With increasing T_g, the PL peak of InAsSb nanostructures shifts to longer wavelength side, which can be mainly explained by the size (height) change in InAsSb islands with increasing T_g. The FWHM of PL peaks also increases somewhat with increasing growth temperature, which can be attributed to the increased size fluctuation of InAsSb nanostructures with increasing T_g, as discussed.

Figure 3 shows the typical AFM images of the InAsSb nanostructures grown under 520 °C at a R_g of 0.33, 0.83, and 1.17 ML/s. All the InAsSb islands obtained have small average heights (1.5, 1.3, and 1.1 nm for the InAsSb islands grown at 0.33, 0.83, and 1.17 ML/s, respectively). Combined

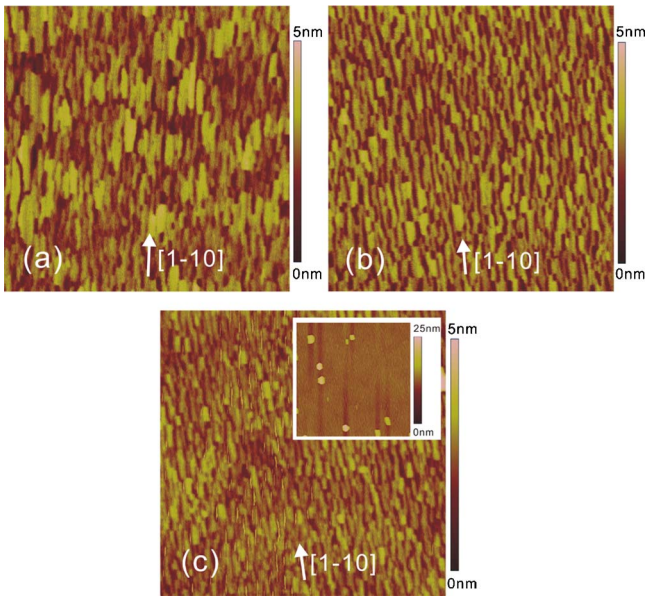

FIG. 3. (Color online) Typical AFM images of InAsSb/InP nanostructures grown at the rate of (a) 0.33 ML/s, (b) 0.83 ML/s, and (c) 1.17 ML/s. AFM scan size is 1 μm^2. The inset of (c) shows an AFM image with scan size of 4 μm^2 of the sample grown with 1.17 ML/s.

with Fig. 1(b), it is noted that the aspect ratio of InAsSb islands changes a lot with varying InAsSb R_g. When the InAsSb R_g increases from 0.33 to 1.17 ML/s, the length of InAsSb islands decreases from 120 to 55 nm, while their widths are all kept at around 25 nm. This decreased aspect ratio with increasing R_g can also be ascribed to the kinetic characteristic of SK growth.[17,18] At low R_g, In adatoms have large migration length and will have much more chances to be incorporated into existing QDs that are more energetically favorable. This leads to the formation of long QDash or QWR structures with relatively large size, large size fluctuation, and low density. However, at high R_g, In adatoms will have much shorter migration length. Thus, the In adatoms deposited will have more chances to form new islands, resulting in the formation of InAsSb islands with relatively small aspect ratio, small size, small size fluctuation, and high density. It should be noted that when the growth rate is too large, such as 1.17 ML/s, not all In adatoms deposited have enough time to migrate away to form new islands though their migration length is even shorter. Therefore, some In adatoms deposited will agglomerate together and form very big InAsSb islands, as shown in the inset of Fig. 3(c). Figure 4 shows the 77 K PL spectra of the InAsSb nanostructures grown under different R_g. Combined with Fig. 1(c), it is observed that the PL peaks are centered at 0.8, 0.793, 0.803, and 0.811 eV with a FWHM of 47, 48, 45, and 42 meV for InAsSb nanostructures grown at 0.33, 0.5, 0.83, and 1.17 ML/s, respectively. Obviously, with increasing R_g from 0.5 to 1.17 ML/s there is a blueshift for the PL peak, which confirms the island size change with increasing R_g as observed in Fig. 3. However, there is no blueshift for the PL peak when the R_g increases from 0.33 to 0.5 ML/s, the reason of which is not very clear yet.

In conclusion, the formation and shape control of InAsSb/InP nanostructures has been investigated in detail. The incorporation of Sb atoms into InAs QDs leads to a dramatic change in the nanostructure morphology due to the surfactant effect of Sb atoms and large strain in the system. Due to the kinetic characteristics of SK growth, both elongated InAsSb QDs (short QDashes) and QWRs (long QDashes) can be obtained by choosing proper growth parameters. Low growth temperature and high growth rate will be helpful for achieving elongated QDs, while high growth temperature and low growth rate are good for growing QWRs and QDashes.

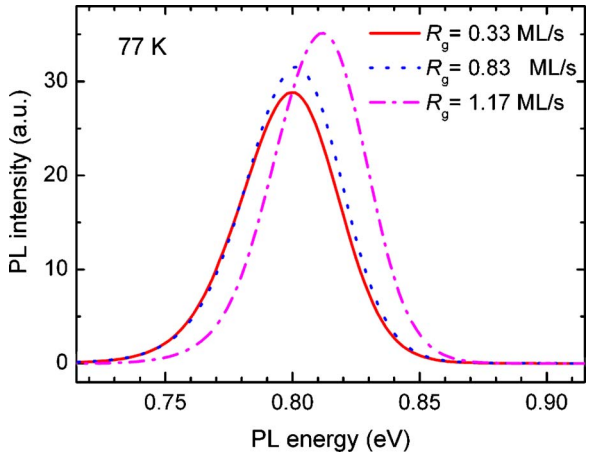

FIG. 4. (Color online) 77 K PL spectra of the InAsSb/InP nanostructures grown at the rate of 0.33, 0.83, and 1.17 ML/s.

Financial support from the Australian Research Council is gratefully acknowledged.

[1]D. Bimberg, M. Grundmann, and N. N. Ledentsov, *Quantum Dot Heterostructures* (Wiley, New York, 1999).
[2]Y. Masumoto and T. Takagahara, *Semiconductor Quantum Dots* (Springer, Berlin, 2002).
[3]T. J. Badcock, R. J. Royce, D. J. Mowbray, M. S. Skolnick, H. Y. Liu, M. Hopkinson, K. M. Groom, and Q. Jiang, Appl. Phys. Lett. **90**, 111102 (2007).
[4]S. G. Li, Q. Gong, Y. F. Lao, K. He, J. Li, Y. G. Zhang, S. L. Feng, and H. L. Wang, Appl. Phys. Lett. **93**, 111109 (2008).
[5]C. Cornet, F. Doré, A. Ballestar, J. Even, N. Bertru, A. Le Corre, and S. Loualiche, J. Appl. Phys. **98**, 126105 (2005).
[6]Y. Qiu and D. Uhl, Appl. Phys. Lett. **84**, 1510 (2004).
[7]F. Doré, C. Cornet, P. Caroff, A. Ballestar, J. Even, N. Bertru, O. Dehaese, I. Alghoraibi, H. Folliot, R. Piron, A. Le Corre, and S. Loualiche, Phys. Status Solidi C **3**, 3920 (2006).
[8]F. Doré, C. Cornet, A. Schliwa, A. Ballestar, J. Even, N. Bertru, O. Dehaese, I. Alghoraibi, H. Folliot, R. Piron, A. Le Corre, and S. Loualiche, Phys. Status Solidi C **3**, 524 (2006).
[9]K. Kawaguchi, M. Ekawa, T. Akiyama, H. Kuwatsuka, and M. Sugawara, J. Cryst. Growth **291**, 154 (2006).
[10]K. Kawaguchi, M. Ekawa, T. Akiyama, H. Kuwatsuka, and M. Sugawara, J. Cryst. Growth **298**, 558 (2007).
[11]S. Barik, H. H. Tan, and C. Jagadish, Nanotechnology **17**, 1867 (2006).
[12]G. B. Stringfellow, *Organometallic Vapor-Phase Epitaxy: Theory and Practice* (Academic, San Diego, 1999).
[13]W. G. Schmidt and F. Bechstedt, Phys. Rev. B **55**, 13051 (1997).
[14]D. J. Eaglesham, F. C. Unterwald, and D. C. Jacobson, Phys. Rev. Lett. **70**, 966 (1993).
[15]J. Tersoff and R. M. Tromp, Phys. Rev. Lett. **70**, 2782 (1993).
[16]O. Suekane, S. Hasegawa, T. Okui, M. Takata, and H. Nakashima, Jpn. J. Appl. Phys., Part 1 **41**, 1022 (2002).
[17]V. G. Dubrovskii, G. E. Cirlin, Y. G. Musikhin, Y. B. Samsonenko, A. A. Tonkikh, N. K. Polyakov, V. A. Egorov, A. F. Tsatsul'nikov, N. A. Krizhanovskaya, V. M. Ustinov, and P. Werner, J. Cryst. Growth **267**, 47 (2004).
[18]R. Songmuang, S. Kiravittaya, M. Sawadsaringkarn, S. Panyakeow, and O. G. Schmidt, J. Cryst. Growth **251**, 166 (2003).